



Analytical solution of MHD flow and heat transfer over a permeable nonlinearly stretching sheet in a porous medium filled by a nanofluid

Habib-Olah Sayehvand*

Department of Mechanical Engineering,
Bu-Ali Sina University,
Hamedan, Iran.
E-mail: hsayehvand@yahoo.com

Amir Basiri Parsa

Department of Mechanical Engineering,
Bu-Ali Sina University,
Hamedan, Iran.
E-mail: amirbparsa@yahoo.com

Abstract

In this paper, the differential transform method and Padé approximation DTM-Padé is applied to obtain the approximate analytical solutions of the MHD flow and heat transfer of a nanofluid over a nonlinearly stretching permeable sheet in porous. The similarity solution is used to reduce the governing system of partial differential equations to a set of nonlinear ordinary differential equations which are then solved by DTM-Padé and validity of our solutions is verified by the numerical results (fourth-order Runge-Kutta scheme with the shooting method). The stretching velocity of sheet is assumed to have a power-law variation with the horizontal distance along the plate. It was shown that the differential transform method (DTM) solutions are only valid for small values of independent variable but the obtained results by the DTM-Padé are valid for the whole solution domain with high accuracy. Finally, the analytical solutions of the problem for different values of the fixed parameters are shown and discussed. Furthermore, it is found that permeability parameter of medium has a greater effect on the flow and heat transfer of a nanofluid than the magnetic parameter.

Keywords. DTM-Padé, MHD, Nanofluid, Nonlinear stretching sheet, Numerical method, Porous medium, Prescribed temperature.

1991 Mathematics Subject Classification.

1. INTRODUCTION

Today, the research in Micro and Nano Fluids becomes one of the hottest areas in engineering. At Micro and Nano scale, conventional ideas of classical fluid mechanics do not apply, and the traditional approaches to fluid mechanics problems need to be changed to correctly reflect the importance of the interaction between a fluid and a solid boundary. Conventional heat transfer fluids, for example oil, water, and

Received: 17 January 2016 ; Accepted: 14 November 2016.

* Corresponding author.

ethylene glycol mixtures, are poor heat transfer fluids because of their poor thermal conductivity. Many attempts have been taken by various investigators during the recent years to enhance the thermal conductivity of these fluids by suspending nano/micro particles in liquids [1, 23, 47, 48]. Researchers have observed that thermal conductivity of nanofluid is much higher than that of the base fluids even for low solid volume fraction of nanoparticles in the mixture [14, 15, 37, 38]. The effect of temperature on thermal conductivity in a model has been considered by Kumar et al. [25]. Patel et al. [39] improved the model given in [25] by incorporating the effect of micro-convection due to particle movement. Nano and micro-fluidics is a new area with significant potential for novel engineering applications, especially for the development of new biomedical devices and procedures [27]. Napoli et al. [33] reviewed applications of nanofluidic phenomena to various nanofabricated devices, in particular those designed for biomolecule transport and manipulation. There has been significant interest in nanofluids. This interest is due to its diverse applications, ranging from laser-assisted drug delivery to electronic chip cooling. Nanofluids are made of ultrafine nanoparticles (<100 nm) suspended in a base fluid, which can be water or an organic solvent. Nanofluids possess superior thermo-physical properties like high thermal conductivity, minimal clogging in flow passages, long term stability and homogeneity. Industrial applications of nanofluid are included in electronics, automotive and nuclear applications. Nanobiotechnology is also a fast developing field of research and application in many domains such as in medicine, pharmacy, cosmetics and agro-industry. Many industrial processes involving nanofluid flow and nanoparticle volume fraction, the diffusing species can be generated / absorbed due to chemical reaction with the ambient fluid which can greatly affect the flow and hence the properties and quality of the final product [45]. Different industrial applications of internal heat generation include the polymer production and the manufacturing of ceramics or glassware, phase change processes, thermal combustion processes, the development of a metal waste from spent nuclear fuel [30]. A review of convective transport in nanofluids was conducted by Buongiorno [8]. Rohni et al. [44] investigated the unsteady flow of a nanofluid over a continuously shrinking surface with wall mass suction. Godson et al. [18] presented the recent experimental and theoretical studies on convective heat transfer in nanofluids, their thermo-physical properties and applications and clarified the challenges and opportunities for future research.

Convective flow in porous media has received the attention of researchers during the last several decades owing to its many applications in mechanical, chemical, and civil engineering. Examples include fibrous insulation, food processing and storage, thermal insulation of buildings, geophysical systems, electro-chemistry, metallurgy, the design of pebble bed nuclear reactors, underground disposal of nuclear or non-nuclear waste, cooling system of electronic devices etc. Excellent reviews of the fundamental theoretical and experimental works can be found in the books by Nield and Bejan [35], Vadasz [50], Vafai [51]. The Cheng–Minkowycz problem [10] was investigated by Nield and Kuznetsov [36] for nanofluid where the model involves the effect of Brownian motion and thermophoresis. The classical problem of free convective flow in a porous medium near a horizontal flat plate was first investigated by Cheng and Chang [11]. Following him ,many researchers such as Chang and Cheng [12], Shiunlin



and Gebhart [49], Merkin and Zhang [31], and Chaudhary et al. [9] have extended the problem in various aspects. Gorla and Chamkha [19] presented a similarity analysis of free convective flow of nanofluid past a horizontal upward facing plate in a porous medium numerically. Khan and Pop [24] extended this problem for nanofluid. Very recently, Aziz et al. [5] extended the same problem for a water-based nanofluid containing gyrotactic microorganisms.

The study of magnetohydrodynamic (MHD) flow has received a great deal of research interest due to its importance in many engineering studies and industries, such as modern metallurgy, plasma studies, the boundary layer control in aerodynamics, MHD power generators, cooling of nuclear reactors, petroleum industries, and crystal growth. Bluman et al. [7] studied MHD stagnation point flow towards a stretching sheet numerically. Their analysis showed that velocity at a point increases with an increase in the magnetic field when the free stream velocity is greater than the stretching velocity. Rashidi et al. [41] presented series solutions for convective heat transfer for a micropolar fluid in the presence of uniform magnetic field. Mukhopadhyay [32] analyzed the effect of magnetic field on MHD boundary layer flow and heat transfer adjacent to an exponentially stretching sheet. Convection heat transfer and fluid flow through porous medium are another important field of research that have many important applications in geophysical fields such as geothermal and petroleum resources. Solid matrix heat exchanges, drying of porous solids, thermal insulation and enhanced oil recovery are some of industrial applications of boundary layer problems in porous medium. Several excellent books and review articles by Nield and Bejan [35] and Aziz and Pop [5] have appeared recently dealing with this area, which review the present understanding of the basic mechanisms involved.

Most scientific problems and phenomena such as boundary-layer problem occur nonlinearly. We have difficulty usually finding their exact analytical solutions. Explicit solutions to the nonlinear equations are of fundamental importance. Except a limited number of these problems that have precise analytical solution, most of them do not have analytical solution, so these nonlinear equations should be solved using other methods. In recent decades, much attempt has been done to the newly developed methods to introduce an analytic solution of these equations. The basic technique that we used is the DTM, which is based on Taylor series expansion. In 1986, Zhou [53] employed the basic ideas of DTM for solving linear and nonlinear problems in electrical circuit problems. It gives exact values of the n_{th} derivative of an analytical function at a point in terms of known and unknown boundary conditions in a fast manner. The differential transform is an iterative procedure for obtaining analytic Taylor series solutions of differential equations. Ayaz [2] applied it to the system of differential equations. Jang et al. [22] presented the two-dimensional DTM for solution of partial differential equations. This method was successfully applied to various application problems [3, 4, 6, 16, 17, 18, 20, 40, 42, 46, 54]. On the other hand, if the DTM is used to solve differential equations with the boundary conditions at infinity, the obtained results will be incorrect (when the boundary-layer variable go to infinity, the obtained series solutions are divergent). In addition, power series aren't useful for large values of η , say $\eta \rightarrow \infty$ (when η is independent variable of problem). Kuznetsov [26] and others have formally shown that power series in isolation



are not useful for handling boundary value problems. This can be attributed to the possibility that the radius of convergence may not be sufficiently large to contain the boundaries of the domain. Therefore, the combination of the series solution through the DTM or any other series solution method with the Padé approximation provides an effective tool for handling boundary value problems on infinite or semi-infinite domains. The MHD boundary-layer flow is investigated by employing the modified Adomian decomposition method (ADM) and the Padé approximation by Liao et al. [28].

Therefore, the present study focuses on using any combination of speed and temperature boundary conditions by employing the most general power-law velocity and temperature distributions considering various working nanofluid with different values of nanoparticle solid volume fraction. In addition, effects of suction/injection, magnetic field and permeability of medium are investigated and discussed. With a similarity transformation, the Navier–Stokes equations have been reduced to a set of nonlinear ordinary differential equations.

The differential transform method and Pade'approximation are applied to solve the ODEs. The validity of our solutions is verified by the numerical results (Runge-Kutta-Fehlberg fourth-fifth order and shooting method). The effect of relevant parameters on dimensionless fluid velocity, temperature, nanoparticle volume fraction is investigated and shown graphically and discussed. The obtained results are then compared with the results of Cortell [13], Rohni et al. [44], Hady et al. [21] and Hamad [20] to support their validity.

2. FORMULATION OF THE PROBLEM

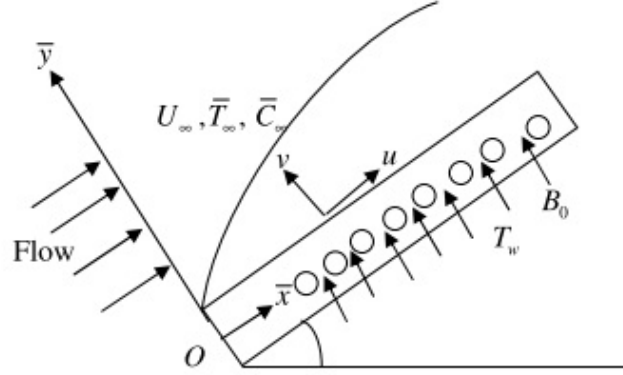
Consider the two-dimensional laminar boundary layer flow of an electrically conducting fluid over a permeable stretching sheet in a porous medium filled by a nanofluid as shown in FIGURE 1. Cartesian coordinates x and y are defined such that the x -axis is measured along the stretching sheet and the y -axis is measured normal to it. It is assumed that the sheet is stretched with the nonlinear velocity $u_w = U_0 x^n$ in a quiescent nanofluid where $U_0 > 0$ is the stretching parameter and n is nonlinear velocity parameter. The surface temperature T_w is assumed to vary as a power-law function of the distance along the plate, i.e., $T_w = T_0 x^m + T_\infty$ where T_0 is the characteristic temperature of the nanofluid and m is nonlinear temperature parameter. It is also assumed that the velocity of the mass transfer is $v_w(x)$ with $v_w(x) > 0$ for suction and $v_w(x) < 0$ for injection, respectively. It is further assumed that the base fluid (i.e. water) and the nanoparticles are in thermal equilibrium and no slip occurs between them. The basic steady conservation of mass, momentum and energy equations for a nanofluid under a vertical magnetic field through porous media are

$$\frac{\partial u}{\partial x} + \frac{\partial v}{\partial y} = 0, \quad (2.1)$$

$$u \frac{\partial u}{\partial x} + v \frac{\partial u}{\partial y} = \nu_{nf} \frac{\partial^2 u}{\partial y^2} - \frac{\nu_{nf}}{K} u - \frac{\sigma B_0^2}{\rho_{nf}} u, \quad (2.2)$$



FIGURE 1. The schematic of the problem and coordinate system.



$$u \frac{\partial T}{\partial x} + v \frac{\partial T}{\partial y} = \alpha_{nf} \frac{\partial^2 T}{\partial y^2}. \quad (2.3)$$

The boundary conditions are taken to be

$$u = u_w(x), \quad v = v_w(x), \quad T = T_w(x) \quad \text{at } y = 0, \quad u \rightarrow 0, \quad T \rightarrow T_\infty, \quad \text{as } y \rightarrow \infty, \quad (2.4)$$

where

$$\frac{k_{nf}}{k_f} = \frac{(k_s + 2k_f) - 2\phi(k_f - k_s)}{(k_s + 2k_f) + \phi(k_f - k_s)}, \quad (\rho C_p)_{nf} = (1 - \phi)(\rho C_p)_f + \phi(\rho C_p)_s, \quad (2.5)$$

$$\mu_{nf} = \frac{\mu_f}{(1 - \phi)^{2.5}}, \quad \rho_{nf} = (1 - \phi)\rho_f + \phi\rho_s, \quad \nu_{nf} = \frac{\mu_{nf}}{\rho_{nf}}, \quad \alpha_{nf} = \frac{k_{nf}}{(\rho C_p)_{nf}}. \quad (2.6)$$

In order to obtain similarity solutions of Eqs. (2.1)-(2.3) with the boundary conditions (2.4), we introduce the following similarity variables

$$\psi = \left(\frac{2\nu_f x u_w}{n+1} \right)^{1/2} f(\eta), \quad \eta = \left(\frac{(n+1)u_w}{2\nu_f x} \right)^{1/2} y, \quad \theta(\eta) = \frac{T - T_\infty}{T_w - T_\infty}, \quad (2.7)$$

where ψ is the stream function defined as $u = \frac{\partial \psi}{\partial y}$ and $v = \frac{\partial \psi}{\partial x}$. Substituting (2.7) into Eqs. (2.1)-(2.3), we obtain the following ordinary differential equations

$$f''' + (1 - \phi)^{2.5} \left(1 - \phi + \frac{\phi \rho_s}{\rho_f} \right) \left\{ f f'' - \frac{2n}{n+1} f'^2 \right\} - \frac{2}{U_0(n+1)} \left\{ (1 - \phi)^{2.5} M + \kappa \right\} f' = 0, \quad (2.8)$$



$$\frac{k_{nf}}{k_f}\theta'' + Pr \left((1 - \phi)(1 + \phi \frac{(\rho C_p)_s}{(\rho C_p)_f}) \right) \left\{ f\theta' - \frac{2m}{n+1} f'\theta \right\} = 0, \tag{2.9}$$

Subject to the boundary conditions

$$f(0) = -f_0\sqrt{\frac{2}{n+1}}, \quad f'(0) = 1, \quad \theta(0) = 1, \quad f'(\infty) \rightarrow 0, \quad \theta(\infty) \rightarrow 0, \tag{2.10}$$

Where $f_0 = \text{Constant}$ if we take $\nu_w = (U_0\nu_f x^n - 1)^{1/2}$. The parameter f_0 is the suction/injection parameter with $f_0 > 0$ and $f_0 < 0$ corresponding to mass injection and mass suction, respectively. The skin friction coefficient C_f and the local Nusselt number Nu_x are the physical quantities of interest which are defined as

$$C_f = \frac{\tau_w}{\rho_f u_\infty^2}, \quad Nu_x = \frac{xq_w}{k_f(T_w - T_\infty)}, \tag{2.11}$$

where

$$\tau_w = \mu_{nf} \left(\frac{\partial u}{\partial y} \right)_{y=0}, \quad q_w = -k_{nf} \left(\frac{\partial T}{\partial y} \right)_{y=0}. \tag{2.12}$$

Substituting (2.7) into Eqs. (2.11) and (2.12), we obtain

$$C_f(Re_x)^{1/2} = \left(\frac{n+1}{2} \right)^{1/2} \frac{f''(0)}{(1-\phi)^{2.5}}, \quad Nu_x(Re_x)^{-1/2} = -\frac{k_{nf}}{k_f} \left(\frac{n+1}{2} \right)^{1/2} \theta'(0), \tag{2.13}$$

Where $Re_x = \frac{u_\infty x}{\nu_f}$ is the local Reynolds number.

3. BASIC IDEA OF THE DTM

Consider a function $u(x)$ which is analytic in a domain T and let $x = x_0$ represent any point in T . The function $u(x)$ is then represented by a power series whose centre is located at x_0 . The differential transform of the function $u(x)$ is given by (see ref [16])

$$U(k) = \frac{1}{k!} \left[\frac{d^k u(x)}{dx^k} \right]_{x=x_0}, \tag{3.1}$$

where $u(x)$ is the original function and $U(k)$ the transformed function. The inverse transformation is defined as follows

$$u(x) = \sum_{k=0}^{\infty} (x - x_0)^k U(k). \tag{3.2}$$

Considering Eq. (3.2), it is noticed that the concept of differential transform is derived from Taylor series expansion. However, this method does not evaluate the derivatives



symbolically. In actual applications, the function $u(x)$ is expressed by a finite series and Eq. (3.1) can be rewritten as follows:

$$u(x) \cong \sum_{k=0}^i (x - x_0)^k U(k). \quad (3.3)$$

Which means that $u(x) = \sum_{k=m+1}^{\infty} (x - x_0)^k U(k)$ is negligibly small. Usually, the value of i is decided by convergence of the series coefficients.

4. THE PADÉ APPROXIMANTS

Suppose that we are given a power series $\sum_{i=0}^{\infty} a_i x^i$, representing a function $f(x)$, so that

$$f(x) = \sum_{i=0}^{\infty} a_i x^i. \quad (4.1)$$

The Padé approximant is a rational fraction and the notation for such a Padé approximant is [41]

$$[L, M] = \frac{P_L(x)}{Q_M(x)}, \quad (4.2)$$

where $P_L(x)$ is a polynomial of degree at most L and $Q_M(x)$ is a polynomial of degree at most M . We have

$$f(x) = a_0 + a_1 x + a_2 x^2 + a_3 x^3 + a_4 x^4 + \dots, \quad (4.3)$$

$$P_L(x) = p_0 + p_1 x + p_2 x^2 + p_3 x^3 + \dots + p_L x^L, \quad (4.4)$$

$$Q_M(x) = q_0 + q_1 x + q_2 x^2 + q_3 x^3 + \dots + q_M x^M, \quad (4.5)$$

Notice that in Eq. (4.2), there are $L+1$ numerator coefficients and $M+1$ denominator coefficients. Since we can clearly multiply the numerator and denominator by a constant and leave $[L, M]$ unchanged, we impose the normalization condition

$$Q_M(0) = 1. \quad (4.6)$$

So, there are $L+1$ independent numerator coefficients and M independent denominator coefficients, making $L+M+1$ unknown coefficients in all. This number suggests that normally the $[L, M]$ ought to fit the power series Eq. (4.1) through the orders $1, x, x^2, \dots, x^{L+M}$. Using the conclusion given in [41], we know that the $[L, M]$ approximant is uniquely determined. In the notation of formal power series,

$$\sum_{i=0}^{\infty} a_i x^i = \frac{p_0 + p_1 x + p_2 x^2 + p_3 x^3 + \dots + p_L x^L}{q_0 + q_1 x + q_2 x^2 + q_3 x^3 + \dots + q_M x^M} + O(x^{L+M+1}). \quad (4.7)$$

small By cross-multiplying Eq. (4.7), we find that

$$\begin{aligned} (a_0 + a_1 x + a_2 x^2 + a_3 x^3 + \dots)(1 + q_1 x + q_2 x^2 + \dots + q_M x^M) \\ = p_0 + p_1 x + p_2 x^2 + p_3 x^3 + \dots + p_L x^L + O(x^{L+M+1}). \end{aligned}$$



(4.8)

From Eq. (4.8), one can obtain the set of equations

$$\begin{cases} a_0 = p_0, \\ a_1 + a_0q_1 = p_1, \\ a_2 + a_1q_1 + a_0q_2 = p_2, \\ \vdots \\ a_L + a_{L-1}q_1 + \dots + a_0q_L = p_L, \end{cases} \tag{4.9}$$

and

$$\begin{cases} a_{L+1} + a_Lq_1 + \dots + a_{L-M+1}q_M = 0, \\ a_{L+2} + a_{L+1}q_1 + \dots + a_{L-M+2}q_M = 0, \\ \vdots \\ a_{L+M} + a_{L+M-1}q_1 + \dots + a_Lq_M = 0. \end{cases} \tag{4.10}$$

Where $a_n = 0$ for $n < 0$ and $q_j = 0$ for $j > M$.

If Eqs. (4.9) and (4.10) are nonsingular, then we can solve them directly

$$[L, M] = \frac{\begin{vmatrix} a_{L-M+2} & a_{L-M+2} & \dots & a_{L+1} \\ \vdots & \vdots & \ddots & \vdots \\ a_L & a_{L+1} & \dots & a_{L+M} \\ \sum_{j=M}^L a_{j-M}x^j & \sum_{j=M-1}^L a_{j-M+1}x^j & \dots & \sum_{j=0}^L a_jx^j \end{vmatrix}}{\begin{vmatrix} a_{L-M+1} & a_{L-M+2} & \dots & a_{L+1} \\ \vdots & \vdots & \ddots & \vdots \\ a_L & a_{L+1} & \dots & a_{L+M} \\ x^M & x^{M-1} & \dots & 1 \end{vmatrix}} \tag{4.11}$$

If the lower index on a sum exceeds the upper, the sum is replaced by zero. Alternate forms are

$$\begin{aligned} [L, M] &= \sum_{j=0}^{L-M} a_jx^j + x^{L-M+1}w_{L/M}^T W_{L/M}^{-1} w_{L/M} \\ &= \sum_{j=0}^{L+n} a_jx^j + x^{L+n+1}w_{(L+1)/M}^T W_{L/M}^{-1} w_{(L+n)/M}, \end{aligned} \tag{4.12}$$

for

$$W_{L,M} = \begin{bmatrix} a_{L-M+1} - xa_{L-M+2} & \dots & a_L - xa_{L+1} \\ \vdots & \ddots & \vdots \\ a_L - xa_{L+1} & \dots & a_{L+M+1} - xa_{L+M} \end{bmatrix}, \tag{4.13}$$

$$w_{L,M} = \begin{bmatrix} a_{L-M+1} \\ a_{L-M+2} \\ \vdots \\ a_L \end{bmatrix}. \tag{4.14}$$

The construction of $[L, M]$ approximants involves only algebraic operations [41]. Each choice of L degree of the numerator and M degree of the denominator, leads to an



approximant. The major difficulty in applying the technique is how to direct the choice in order to obtain the best approximant. This needs the use of a criterion for the choice depending on the shape of the solution. We construct the approximants using Mathematica software in the following sections. More importantly, the diagonal approximant is the most accurate approximant; therefore, we will construct only the diagonal approximants in the following discussions.

5. ANALYTICAL APPROXIMATIONS BY MEANS OF THE DTM PADÉ

The fundamental mathematical operations performed by DTM are listed in Table 1. Taking differential transform of Eqs. (2.8), (2.9), we obtain

$$\begin{aligned} & (k+1)(k+2)(k+3)F[k+3]+ \\ & (1-\phi)^{2.5}(1-\phi+\phi\rho_s/\rho_f)(\sum_{r_1=0}^k[F[r_1](k+2-r_1)(k+1-r_1)F[k+2-r_1]]- \\ & \frac{2n}{n+1}\sum_{r_1=0}^k[Fr_1+1(k+1-r_1)F[k+1-r_1]])- \\ & \frac{2}{U_0(n+1)}\{(1-\phi)^{2.5}M+\kappa\}(k+1)F[k+1]=0, \end{aligned} \quad (5.1)$$

$$\begin{aligned} & \frac{k_n f}{k_f}(k+1)(k+2)\Theta[k+2]+Pr\left((1-\phi)\left(1+\phi\frac{(\rho C_p)_s}{(\rho C_p)_f}\right)\right) \\ & (\sum_{r_1=0}^k[F[r_1](k+1-r_1)\Theta[k+1-r_1]]) \quad (5.2) \\ & -\frac{2m}{n+1}\sum_{r_1=0}^k[\Theta[r_1](k+1-r_1)F[k+1-r_1]]=0, \end{aligned}$$

where $F(k)$ and $\Theta(k)$ are the differential transform of $f(\eta)$ and $\theta(\eta)$, respectively. By applying the DTM into Eq. (2.10), differential transform of boundary conditions is thus determined into a recurrence equation that finally leads to the solution of a system of algebraic equations. As for a problem with the boundary conditions at the infinity, differential transform of infinity boundary conditions is indeterminate; thus, we must consider the boundary conditions (Eqs. (2.10)) as follows

$$\begin{aligned} f(0) &= -f_0\sqrt{\frac{2}{(n+1)}}, \quad f'(0) = 1, \quad f''(0) = \alpha, \\ \theta(0) &= 1, \quad \theta'(0) = \omega. \end{aligned} \quad (5.3)$$

Therefore, problem changes to an initial conditions problem. The differential transform of the boundary conditions is as follows

$$\begin{aligned} F(0) &= -f_0\sqrt{\frac{2}{(n+1)}}, \quad F(1) = 1, \quad F(2) = \frac{\alpha}{2}, \\ \Theta(0) &= 1, \quad \Theta(1) = \omega. \end{aligned} \quad (5.4)$$

Moreover, substituting Eqs. (5.4) into Eqs. (5.1), (5.2) and by recursive method, we can calculate other values of $F[k]$ and $\Theta[k]$. Hence, substituting all $F[k]$, $\Theta[k]$ into Eq. (3.3), the series solutions are obtained. After the series solutions are found, the



Padé approximation [41, 43] must be applied. Using asymptotic boundary condition ($f'(\infty) \rightarrow 0$, $\theta(\infty) \rightarrow 0$), we can obtain α and ω . For analytical solution, the convergence analysis was performed and in Eq. (4.2), the i value is selected equal to 50. After the DTM solutions were found, the Padé approximant must be applied. The order of Padé approximation is selected as a reason to agreeable accuracy of solution; on the other hand, if the order of Padé approximation increases, the accuracy of the solution increases. For example, election of cu as nanoparticle in the water and $\phi = 0.1$, $n = 2.0$, $U_0 = 1.0$, $M = 1.0$, $\kappa = 0.1$, $Pr = 6.2$, $m = 4.0$ and $f_0 = 0.1$ and suitable order of Padé approximation $[L, M]$ lead to the analytical solutions as follows:

$$f'(\eta)_{[10,10]} \approx (1.0 + 0.824767\eta - 0.0450612\eta^2 - 0.212118\eta^3 - 0.0065524\eta^4 + 0.028038\eta^5 - 0.00158693\eta^6 - 0.00389942\eta^7 + 0.00142907\eta^8 - 0.00028584\eta^9 + 0.0000133662\eta^{10}) / (1.0 + 3.39521\eta + 5.30164\eta^2 + 5.02857\eta^3 + 3.23024\eta^4 + 1.48195\eta^5 + 0.497618\eta^6 + 0.12268\eta^7 + 0.0217099\eta^8 + 0.00257913\eta^9 + 0.000166409\eta^{10}), \quad (5.5)$$

$$\theta(\eta)_{[10,10]} \approx (1.0 + 1.00464\eta + 2.80042\eta^2 + 0.948566\eta^3 + 1.59213\eta^4 - 0.220317\eta^5 + 0.228846\eta^6 - 0.209529\eta^7 + 0.0612429\eta^8 - 0.00885532\eta^9 + 0.000495686\eta^{10}) / (1.0 + 3.93975\eta + 8.81264\eta^2 + 13.2084\eta^3 + 13.6918\eta^4 + 10.0885\eta^5 + 5.39006\eta^6 + 2.09237\eta^7 + 0.57634\eta^8 + 0.104508\eta^9 + 0.00971635\eta^{10}). \quad (5.6)$$

6. COMPARISONS AND VERIFICATION

It is worth citing that for impermeable medium ($\kappa = 0$) and in the absence of magnetic field ($M = 0$) and solid volume fraction ($\phi = 0$) our problem reduces to Refs. [13, 20, 21, 44]. The results for the skin friction coefficient and the local Nusselt are compared with those reported in Refs [13, 20, 21, 44] for different values of n and f_0 when $Pr = 1.0$ and $m = 2n$ (Table 2). The thermophysical properties of the base fluid and the nanoparticles are listed in Table 3. Also, we compared our results with those given by Hamad [20] for different values of ϕ and M and for three different types of nanoparticle in the water when $f_0 = \kappa = m = 0.0$, $U_0 = n = 1.0$, $pr = 6.2$ (Table 4). The quantitative comparisons are found to be in excellent agreement and thus give confidence that the numerical results obtained are accurate.

7. RESULTS AND DISCUSSION

Graphical representation of results is very useful to discuss the physical features presented by the solutions. This section describes the influence of some interesting parameters on the velocity and temperature fields. Similarity Eqs. (2.8) and (2.9) with boundary conditions in Eq. (2.10) were solved analytically by DTM-Padé and numerically using Runge–Kutta fourth order method along with shooting technique. FIGURES 2 and 3 show the profiles $f'(\eta)$ and $\theta(\eta)$ obtained by the DTM-Padé with



various values of L and M (Padé parameters) in comparison with the simple DTM and numerical solutions obtained by the fourth-order Runge-Kutta method respectively, for cu as nanoparticle in the water and $\phi = 0.1$, $n = 2.0$, $U_0 = 1.0$, $M = 1.0$, $\kappa = 0.1$, $Pr = 6.2$, $m = 4.0$ and $f_0 = 0.1$. It is observed that the results of suitable order of Padé approximation $[L, M]$ are very close to the numerical solutions which confirm the validity of these methods. Also, it can be concluded that obtained results by the DTM are only valid for small values of independent variable (η) but the results obtained by the DTM-Padé have good agreement with the numerical results for all values of η . In the following figures, the effects of various physical parameters on the dimensionless velocity and temperature profiles will be investigated. These results have been obtained by the 50th order of the DTM with suitable order of Padé approximation and have been validated by numerical results. FIGURES 4 and 5, respectively, represent that the comparison of solutions of $f'(\eta)$ and $\theta(\eta)$ for fix values $\phi = 0.1$, $n = 2.0$, $U_0 = 1.0$, $M = 1.0$, $\kappa = 0.1$, $Pr = 6.2$, $m = 4.0$ and different values of suction/ injection parameter f_0 . It is observed that the temperature is greater in status of injection than suction but velocity of the fluid does not vary sensibly (FIGURE 5). The effects of the nanoparticle volume fraction ϕ are depicted in FIGURES 6 and 7, when $f_0 = 0.1$, $n = 2.0$, $U_0 = 1.0$, $M = 1.0$, $\kappa = 0.1$, $Pr = 6.2$, $m = 4.0$. If ϕ increases, $f'(\eta)$ and specially $\theta(\eta)$ increase.

The dimensionless velocity and dimensionless temperature profiles for different values of nonlinear velocity parameter n with constant values $f_0 = 0.1$, $\phi = 0.1$, $U_0 = 1.0$, $M = 1.0$, $\kappa = 0.1$, $Pr = 6.2$, $m = 4.0$ are presented in FIGURES 8 and 9. It is observed that the velocity of the fluid decreases with the increase of n but temperature increases extremely. In FIGURES 10 and 11, respectively, comparison of solutions of $f'(\eta)$ and $\theta(\eta)$ for $f_0 = 0.1$, $\phi = 0.1$, $n = 2.0$, $M = 1.0$, $\kappa = 0.1$, $Pr = 6.2$, $m = 4.0$ and different values of stretching velocity coefficient U_0 are shown. As the stretching velocity coefficient increases, the velocity distribution $f'(\eta)$ increases while temperature $\theta(\eta)$ decreases. The dimensionless velocity and dimensionless temperature profiles for different values of magnetic field parameter M with constant values $f_0 = 0.1$, $\phi = 0.1$, $n = 2.0$, $U_0 = 1.0$, $\kappa = 0.1$, $Pr = 6.2$, $m = 4.0$ are presented in FIGURES 12 and 13. It is observed that the velocity of the fluid decreases with the increase of magnetic parameter, and the value of temperature profiles increase with the increase of magnetic parameter. FIGURE 14 presents velocity profiles for different values of permeability parameter of medium κ when $f_0 = 0.1$, $\phi = 0.1$, $n = 2.0$, $U_0 = 1.0$, $M = 1.0$, $Pr = 6.2$, $m = 4.0$. It is obvious that velocity decreases at each point with the increasing values of permeability parameter of medium κ . FIGURE 15 shows the temperature increases as κ increases. It is expected that presence of porous medium causes higher restriction to the fluid, thus the flow becomes slower and reduces the velocity boundary layer thickness and enhances the temperature. The effects of the Prandtl number on the $f'(\eta)$ and $\theta(\eta)$ obtained by the DTM-Padé and numerical solutions, are depicted in FIGURES 16 and 17, respectively, for fixed values $f_0 = 0.1$, $\phi = 0.1$, $n = 2.0$, $U_0 = 1.0$, $M = 1.0$, $\kappa = 0.1$, $m = 4.0$. It is clear that with increase of Prandtl number $\theta(\eta)$ decreases extremely (FIGURE 17), but there is no effect on the velocity $f'(\eta)$ (FIGURE 16). This is in agreement with the physical fact that the thermal boundary-layer thickness



decreases with the increasing Pr . Ultimately, FIGURES 18 and 19 depict the effect of temperature exponent parameter m on velocity and temperature functions when $f_0 = 0.1$, $\phi = 0.1$, $n = 2.0$, $U_0 = 1.0$, $M = 1.0$, $\kappa = 0.1$, $Pr = 6.2$. It is seen that with an increase in the temperature exponent parameter, the velocity does not change prominently whereas the temperature decreases extremely. In FIGURES 4-19, the comparison of the solutions obtained by the DTM-Padé and numerical method show that the results obtained by the DTM-Padé have good agreement with the numerical results for all values of η .

These figures show that the boundary conditions (9) are satisfied and approached infinity asymptotically. Also, FIGURES 20 and 21 show the effects of the type of nanoparticle on velocity and temperature profiles, respectively. It is seen that the highest velocity is achieved for Al_2O_3 working fluid (FIGURE 20). FIGURE 21 shows that the highest temperature is achieved for Cu . It is noted that the Cu nanoparticles have high values of thermal diffusivity; therefore, this increases the temperature which will affect the performance of Cu fluid. It is expected that presence of porous medium causes higher restriction to the fluid, thus, the flow becomes slower, reduces the velocity boundary layer thickness and enhances the temperature.

8. CONCLUSIONS

This paper studied the magnetohydrodynamics flow and heat transfer of a nanofluid over a nonlinearly stretching permeable sheet in porous medium. The surface temperature T_w is assumed to vary as a power-law function of the distance along the plate. The governing partial differential equations have been transformed by a similarity transformations developed by Lie group analysis into a system of ordinary differential equations, which are solved analytically by DTM-Padé and numerical method small (fourth-order Runge-Kutta scheme with the shooting method). The DTM combined with Padé approximants are also shown to be a promising tool in solving two-point boundary value problems consisting of systems of nonlinear differential equations. Without using Padé approximation, the analytical solution obtained by the DTM, can't satisfy boundary conditions at infinity. The effects of the governing parameters f_0 , ϕ , n , U_0 , M , κ , Pr and m and the type of nanoparticle on the fluid flow and heat transfer characteristics are investigated and discussed.

From the present investigation, it may be concluded that:

- (i) The velocity $f'(\eta)$ increases with the increasing ϕ , U_0 and decreases with the increasing n , M and κ .
- (ii) The temperature $\theta(\eta)$ increases with ϕ , n , M , κ and decreases with U_0 , Pr , m .
- (iii) Parameters of Pr , f_0 and m do not affect velocity profile.
- (iv) The temperature is greater in status of injection than suction.

Overall, the DTM-Padé approach again demonstrates very good correlation with the established numerical quadrature (shooting) method, and therefore provides a very useful benchmark for computational techniques such as finite differences[52], finite elements [29] and network electrical simulation methods [34]. As discussed, nonlinear stretching velocity is a fact in industrial applications and we can control the nanofluid



flow and heat transfer in such processes by changing in the various pertinent parameters. Finally, the agreement between analytical and numerical results of the present study with previous published results is excellent.

REFERENCES

- [1] E. Abu-Nada, F. O. Hakan, I. Pop, *Buoyancy induced flow in a nanofluid filled enclosure partially exposed to forced convection*, Superlattices and Microstructures, 51 (2012), 381–395 .
- [2] F. Ayaz, *Solutions of the systems of differential equations by differential transform method*, Applied Mathematics and Computation, 147 (2004), 547–567.
- [3] A. A. Avramenko, S. G. Kobzar , I. V. Shevchuk , A. V. Kuznetsov , L. T.e Iwanisov , *Symmetry of turbulent boundary-layer flows: Investigation of different eddy viscosity models*, Acta Mechanica, 151 (2001), 1–14.
- [4] A. Aziz, M. J. Uddin, M. A. A. Hamad, A. I. M. Ismail, *MHD flow over an inclined radiating plate with the temperature dependent thermal conductivity, variable reactive index and heat generation*, Heat transfer Asian Research, (2012). DOI 10.1002/htj.20409.
- [5] A. Aziz, W.A. Khan, I. Pop, *Free convection boundary layer flow past a horizontal flat plate embedded in porous medium filled by nanofluid containing gyrotactic microorganisms*, International Journal of Thermal Sciences, In press(2012), 1-10.
- [6] A. Aziz, *A similarity solution for laminar thermal boundary layer over flat plate with convective surface boundary condition*, Commun. Nonlinear Sci. Numer. Simul,14 (2009), 1064-1068.
- [7] G. W. Bluman, S. C. Anco, *Symmetry and Integration Methods for Differential Equations*, New York, Springer; (2009).
- [8] J. Buongiorno, *Convective transport in nanofluids*, ASME J. Heat Transf. 128 (2006), 240–250.
- [9] M. A. Chaudhary, J. H. Merkin, I. Pop, *Natural convection from a horizontal permeable surface in a porous medium—numerical and asymptotic solutions*, Transp. Porous Media, 22 (1996) ,327–344.
- [10] P. Cheng, W. J. Minkowycz, *Free convection about a vertical flat plate embedded in a porous medium with application to heat transfer from a dike*, Geophys. Res. , 82 (1977), 2040–2044.
- [11] P. Cheng, I.D. Chang, *Buoyancy induced flows in a saturated porous medium adjacent to impermeable horizontal surfaces*, Int. J. Heat Mass Transf. , 19 (1976), 1267–1272.
- [12] I. D. Chang, P. Cheng, *Matched asymptotic expansions for free convection about an impermeable horizontal surface in a porous medium*, Int. J. Heat Mass Transf. , 26 (1983), 163–173.
- [13] R. Cortell, *Viscous flow and heat transfer over a nonlinearly stretching sheet*, Applied Mathematics and Computation, 184 (2007), 864–873.
- [14] S. K. Das, N. Putra, P. Thiesen, W. Roetzel, *Temperature dependence of thermal conductivity enhancement for nanofluids*, J. Heat Transfer, 125 (2003), 567–574.
- [15] J. A. Eastman, S. U. S. Choi, S. Li, W. Yu, L. J. Thompson, *Anomalously increased effective thermal conductivities of ethylene glycol-based nanofluids containing copper nanoparticles*,



Appl. Phys. Lett. , 78 (2001), 718-720.

- [16] E. Erfani, M. M. Rashidi, A. Basiri parsia, *The modified Differential Transform Method for solving off-centered stagnation flow towards a rotating disc*, International Journal of Computational Methods, 7(4) (2010), 655–670.
- [17] S. K. Ghosh, O. Anwar Bég, J. Zueco, V. R. Prasad, *Transient hydromagnetic flow in a rotating channel permeated by an inclined magnetic field with magnetic induction and Maxwell displacement current effects*, ZAMP: J. Applied Mathematics and Physics, 61 (2010), 147-169.
- [18] L. B. Godson, D. Raja, L. D. Mohan, S. Wongwisesc, *Enhancement of heat transfer using nanofluids*, An overview, Renewable and Sustainable Energy Reviews, 14 (2010), 629–641.
- [19] R. S. R. Gorla, A. Chamkha, *Natural convective boundary layer flow over a horizontal plate embedded in a porous medium saturated with a nanofluid*, J. of Modern Phys., 2 (2011), 62-71.
- [20] M. A. A. Hamad, M. J. Uddin, A. I. M. Ismail, *Radiation effects on heat and mass transfer in MHD stagnation-point flow over a permeable flat plate with thermal convective surface boundary condition, temperature dependent viscosity and thermal conductivity*, Nuclear Engineering and Design, 242 (2012), 194-200.
- [21] F. M. Hady, F. M. Ibrahim, S. M. Abdel-Gaied, M. R. Eid, *Radiation effect on viscous flow of a nanofluid and heat transfer over a nonlinearly stretching sheet*, Nanoscale Res Lett, 7 (2012), 299-308.
- [22] M. J. Jang, C. L. Chen, Y. C. Liu, *Two-dimensional differential transform for partial differential equations*, Applied Mathematics and Computation, 121 (2001), 261–270.
- [23] S. Kakac, A. Pramuanjaroenkij, *Review of convective heat transfer enhancement with nanofluids*, Int. J. Heat Mass Transfer, 52 (2009), 3187–3196.
- [24] W. A. Khan, I. Pop, *Free convection boundary layer flow past a horizontal flat plate embedded in a porous medium filled with a nanofluid*, ASME J. of Heat Trans, 133 (2011). DOI:10.1115/1.4003834.
- [25] D. H. Kumar, H. E. Patel, V. R. R. Kumar, T. Sundararajan, T. Pradeep, S. K. Das, *Model for conduction in nanofluids*, Phys. Rev. Lett., 93 (2004), 144301-1–144301-3.
- [26] A. V. Kuznetsov, A. A. Avramenko, P. Geng, *Analytical investigation of a falling plume caused by bioconvection of oxytactic bacteria in a fluid saturated porous medium*, International Journal of Engineering Science, 42 (2004), 557–569.
- [27] A. V. Kuznetsov, *Non-oscillatory and oscillatory nanofluid bio-thermal convection in a horizontal layer of finite depth*, European Journal of Mechanics B/Fluids, 30 (2011), 156–165.
- [28] S. J. Liao, *An optimal homotopy-analysis approach for strongly nonlinear differential equations*, Commun Nonlinear Sci Numer Simul, 15 (2010), 2003–2006.
- [29] S. J. Liao, *The proposed homotopy analysis technique for the solution of nonlinear problems*, 1992. Thesis(Ph.D.) Shanghai Jiao Tong University.
- [30] O. D. Makind, A. Aziz, *Mixed Convection From a Convectively Heated Vertical Plate to a Fluid With Internal Heat Generation*, Journal of Heat Transfer, 133 (2011), 122501-1.



- [31] J. H. Merkin, G. Zhang, *On the similarity solutions for free convection in a saturated porous medium adjacent to impermeable horizontal surfaces*, *Warme-und Stoffubertr.*, 25 (1990), 179–184.
- [32] S. Mukhopadhyay, G. C. Layek, *Effects of variable fluid viscosity on flow past a heated stretching sheet embedded in a porous medium in presence of heat source/sink.*, *Meccanica*, 2011. DOI 10.1007/s11012-011-9457-6.
- [33] M. Napoli, J. C. T. Eijkel, S. Pennathur, *Nanofluidic technology for biomolecule applications: a critical review*, *Lab on a Chip*, 10 (2010), 957–985.
- [34] A. H. Nayfeh, *Perturbation methods*, New York, Wiley, 2000.
- [35] D. A. Nield, A. Bejan, *Convection in Porous Media*, 3rd ed., Springer, 2006.
- [36] D. A. Nield, A. V. Kuznetsov, *The Cheng–Minkowycz problem for the double-diffusive natural convective boundary layer flow in a porous medium saturated by a nanofluid*, *Int. J. of Heat and Mass Transf.*, 54 (2011), 374–378.
- [37] D. A. Nield, A. V. Kuznetsov, *The Cheng–Minkowycz problem for natural convective boundary-layer flow in a porous medium saturated by a nanofluid*, *Int. J. Heat Mass Trans.*, 52 (2009), 5792–5795.
- [38] D. A. Nield, A. V. Kuznetsov, *The Cheng–Minkowycz problem for the double-diffusive natural convective boundary layer flow in a porous medium saturated by a nanofluid*, *Int. J. of Heat and Mass Transf.*, 54 (2011), 374–378.
- [39] H. E. Patel, T. Sundarajan, T. Pradeep, A. Dasgupta, N. Dasgupta, S. K. Das, *A micro-convection model for thermal conductivity of nanofluid*, *Pramana J. Phys.*, 65 (2005), 863–869.
- [40] M. M. Rashidi, G. Domairry, S. Dinarvand, *Approximate solutions for the Burger and regularized long wave equations by means of the homotopy analysis method*, *Communications in Nonlinear Science and Numerical Simulation*, 14 (2009), 708–717.
- [41] M. M. Rashidi, N. Laraqi, A. Basiri Parsa, *Analytical Modeling of heat convection in magnetized micropolar fluid by using modified differential transform method*, *Heat Transfer-Asian Research*, 40(3) (2011), 187–204.
- [42] M. M. Rashidi, S. A. Mohimani Pour, T. Hayat, S. Obaidat, *Analytic approximate solutions for steady flow over a rotating disk in porous medium with heat transfer by homotopy analysis method*, *Computers & Fluids*, 54 (2012), 1–9.
- [43] S. Rawat, R. Bhargava, O. Anwar Bég, *Transient magneto-micropolar free convection heat and mass transfer through a non-Darcy porous medium channel with variable thermal conductivity and heat source effects*, *Proc. IMechE Part C-J, Mechanical Engineering Science*, 223 (2009), 2341–2355.
- [44] A. M. Rohni, S. Ahmad, I. Pop, *Flow and heat transfer over an unsteady shrinking sheet with suction in nanofluids*, *Int. J. Heat Mass Transfer*, 55(7) (2012), 1888–1895.
- [45] A. Z. Sahin, *Transient heat conduction in semi-infinite solid with spatially decaying exponential heat generation*, *Int. Comm. Heat Mass Transfer*, 19 (1992), 349–358.



- [46] M. Sajid, T. Hayat, S. Asghar, *Comparison between the HAM and HPM solutions of thin film flows of non-Newtonian fluids on a moving belt*, *Nonlinear Dynam*, 50 (2007), 27-35.
- [47] R. Seshadri, T. Y. Na, *Group Invariance in Engineering Boundary Value Problems*, New York, Springer, 1985.
- [48] D. Shang, *Theory of Heat Transfer with Forced Convection Film Flows*, *Heat and Mass Transfer*, 3 (2010).
- [49] D. S. Shiunlin, B. Gebhart, *Buoyancy-induced flow adjacent to a horizontal surface submerged in porous medium saturated with cold water*, *Int. J. Heat Mass Transf*, 29 (1986), 611-623.
- [50] P. Vadasz, *Emerging Topics in Heat and Mass Transfer in Porous Media*, Springer, New York, 2008.
- [51] K. Vafai, *Porous Media: Applications in Biological Systems and Biotechnology*, CRC Press, New York, 2010.
- [52] A. S. Warke, S. K. Das, O. Anwar Bég, H. S. Takhar, T. A. Bég, *Numerical modeling of transient mass transfer in an aquifer with simultaneous first order chemical reaction and second order decay using the ADI scheme*, *Int. J. Fluid Mechanics Research*, 35(2) (2008), 105-126.
- [53] J. K. Zhou, *Dierential Transformation and Its Applications for Electrical Circuits*, Huazhong University Press, Wuhan, China, 1986(in Chinese).
- [54] Y. Xuan, Q. Li, *Heat transfer enhancemen of nanofluids*, *Int. J. Heat Fluid Flow*, 21 (2000), 58-64.



FIGURE 2. Comparison between the numerical, DTM and the DTM-padé solution of $f'(\eta)$ for different values of Padé parameters and cu as nanoparticle in the water.

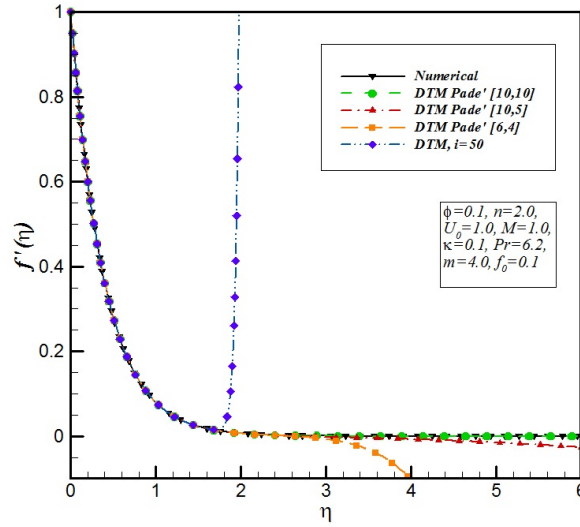


FIGURE 3. Comparison between the numerical, DTM and the DTM-padé solution of $\theta(\eta)$ for different values of Padé parameters and cu as nanoparticle in the water.

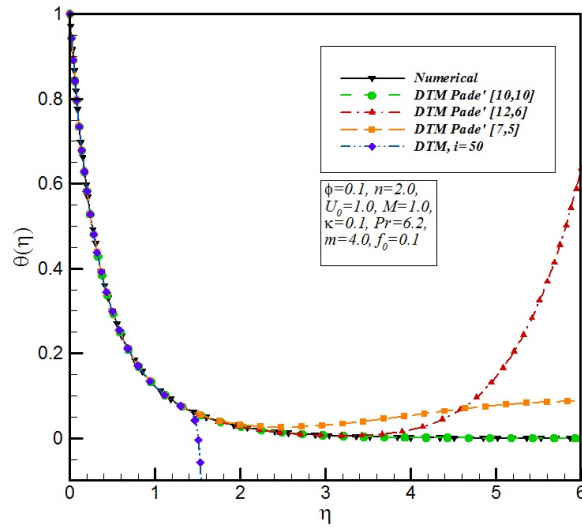


FIGURE 4. Effect of suction/injection parameter f_0 on the dimensionless velocity profile obtained by the DTM-padé and numerical method.

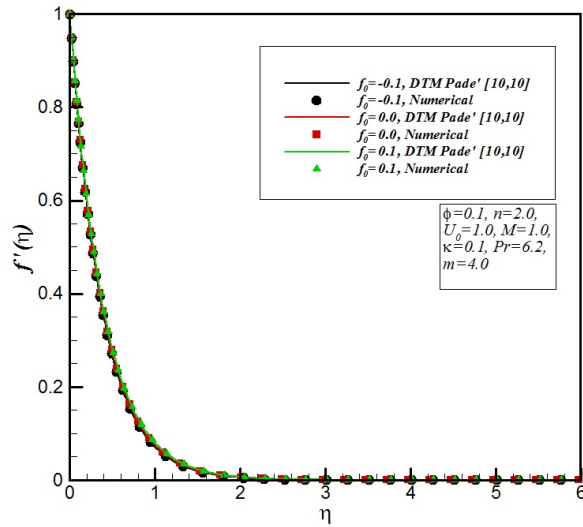


FIGURE 5. Effect of suction/injection parameter f_0 on the dimensionless velocity profile obtained by the DTM-padé and numerical method.

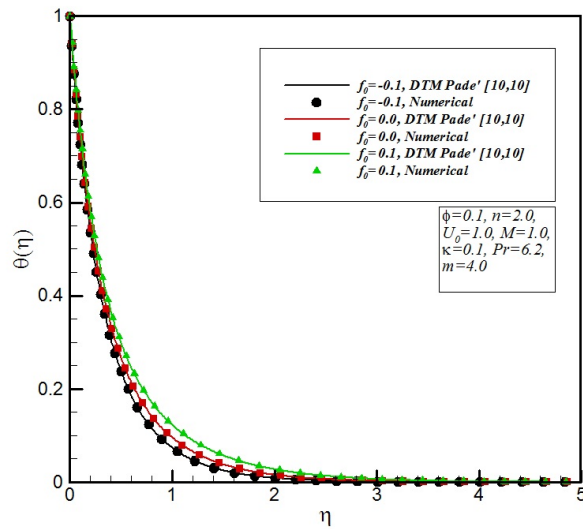


FIGURE 6. Effect of nanoparticle volume fraction ϕ on the dimensionless velocity profile obtained by the DTM-padé and numerical method.

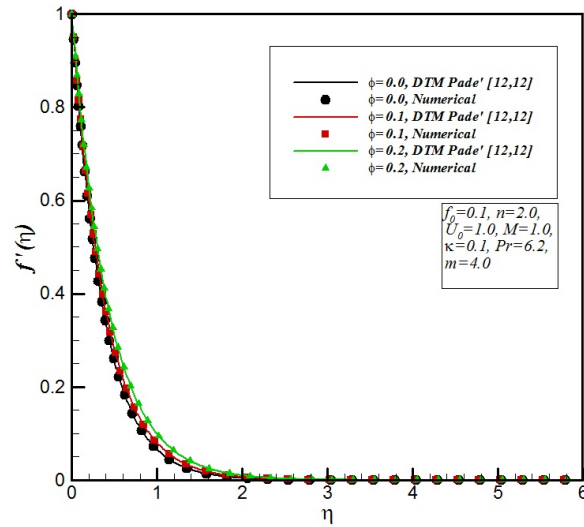


FIGURE 7. Effect of nanoparticle volume fraction ϕ on the dimensionless temperature profile obtained by the DTM-padé and numerical method.

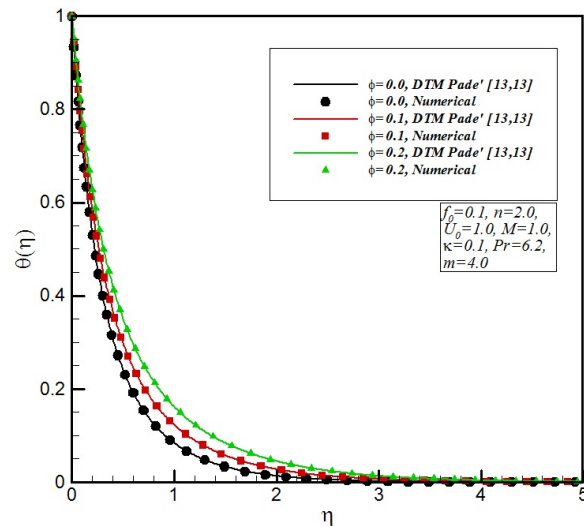


FIGURE 8. Effect of nonlinear velocity parameter n on the dimensionless velocity profile obtained by the DTM-padé and numerical method.

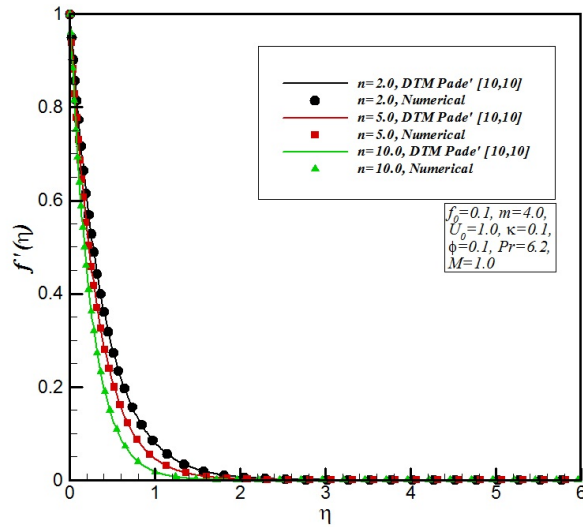


FIGURE 9. Effect of nonlinear velocity parameter n on the dimensionless temperature profile obtained by the DTM-padé and numerical method.

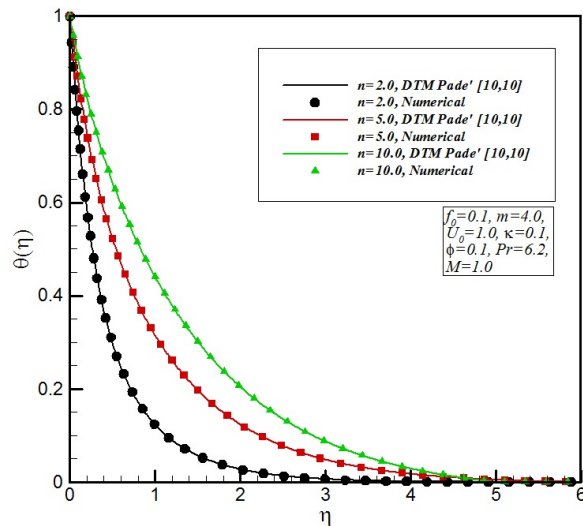


FIGURE 10. Effect of stretching velocity coefficient U_0 on the dimensionless velocity profile obtained by the DTM-padé and numerical method.

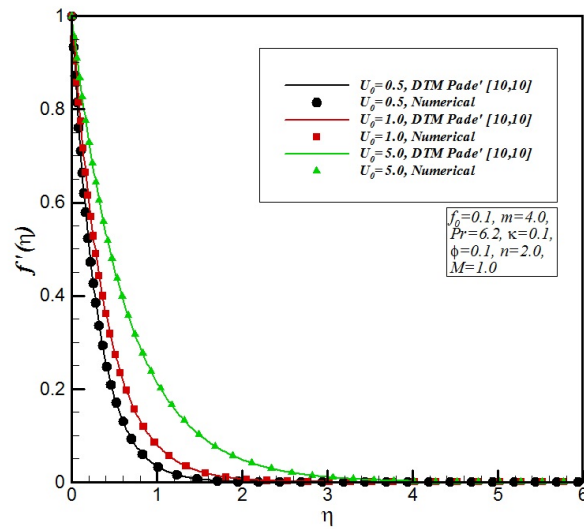


FIGURE 11. Effect of stretching velocity coefficient U_0 on the dimensionless temperature profile obtained by the DTM-padé and numerical method.

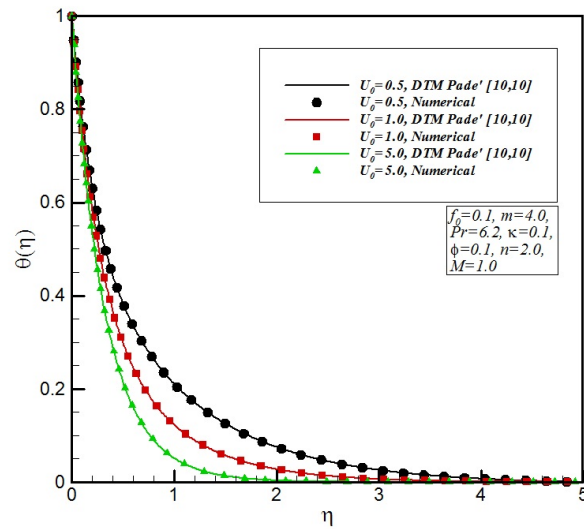


FIGURE 12. Effect of magnetic field parameter M on the dimensionless velocity profile obtained by the DTM-padé and numerical method.

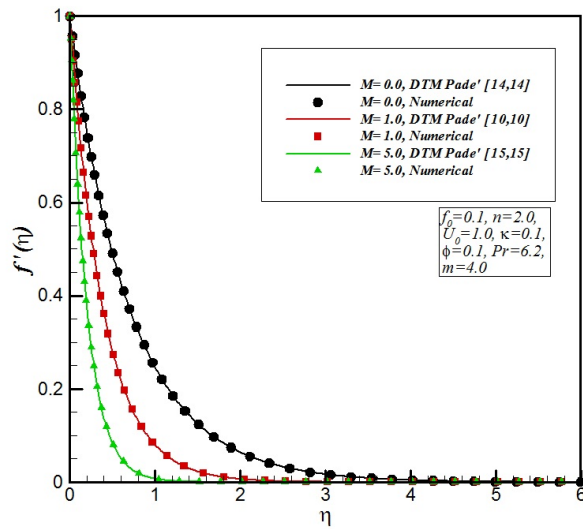


FIGURE 13. Effect of magnetic field parameter M on the dimensionless temperature profile obtained by the DTM-padé and numerical method.

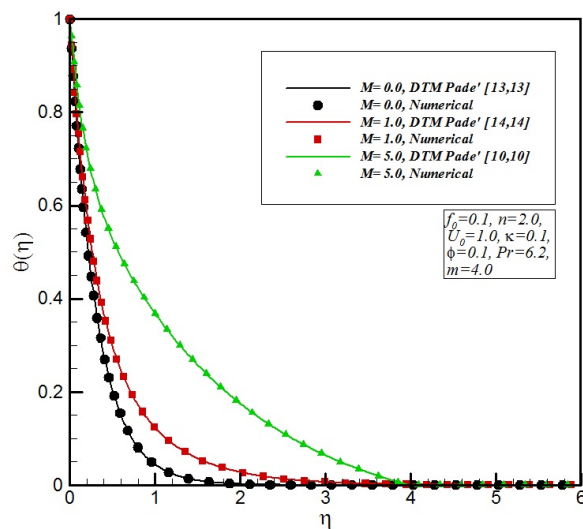


FIGURE 14. Effect of permeability parameter of medium κ on the dimensionless velocity profile obtained by the DTM-padé and numerical method.

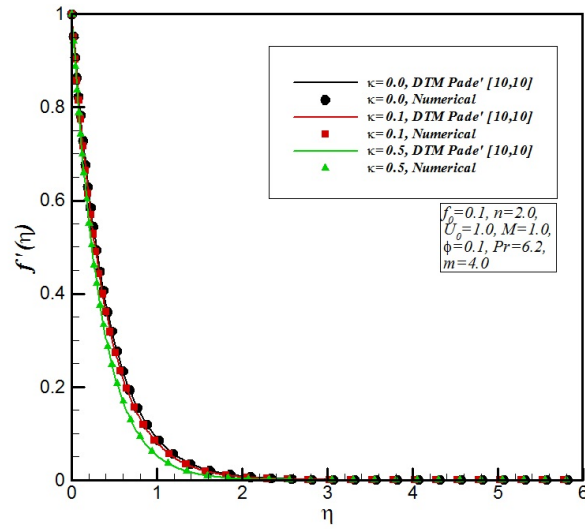


FIGURE 15. Effect of permeability parameter of medium κ on the dimensionless temperature profile obtained by the DTM-padé and numerical method.

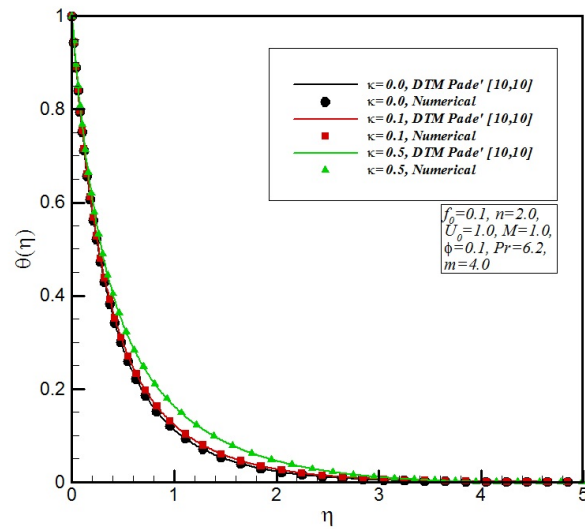


FIGURE 16. Effect of Prandtl number Pr on the dimensionless velocity profile obtained by the DTM-padé and numerical method.

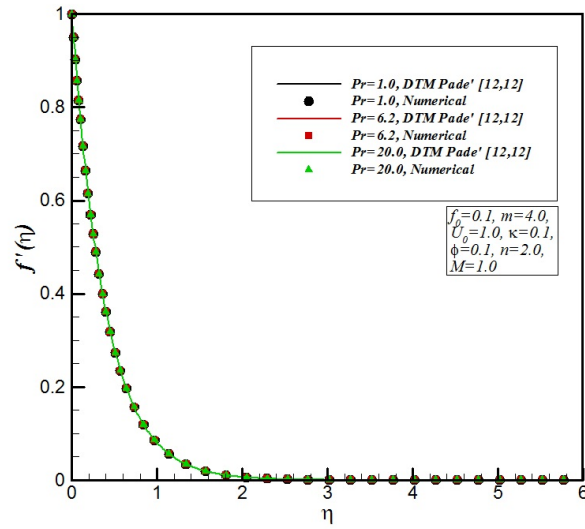


FIGURE 17. Effect of Prandtl number Pr on the dimensionless temperature profile obtained by the DTM-padé and numerical method.

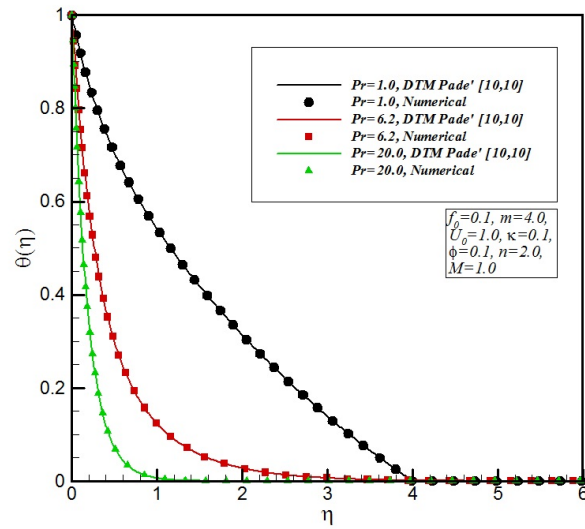


FIGURE 18. Effect of temperature exponent parameter m on the dimensionless velocity profile obtained by the DTM-padé and numerical method.

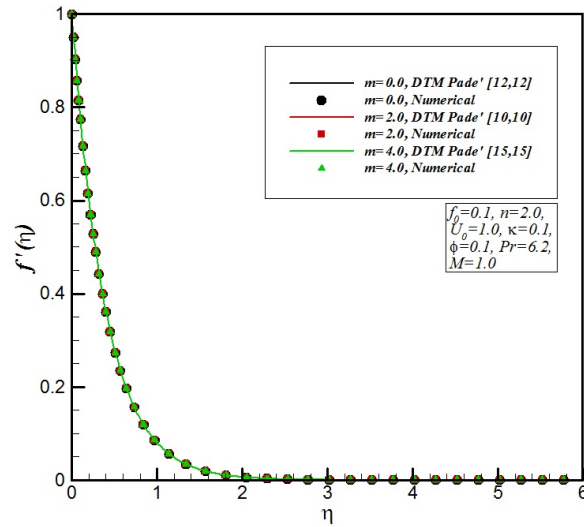


FIGURE 19. Effect of temperature exponent parameter m on the dimensionless temperature profile obtained by the DTM-padé and numerical method.

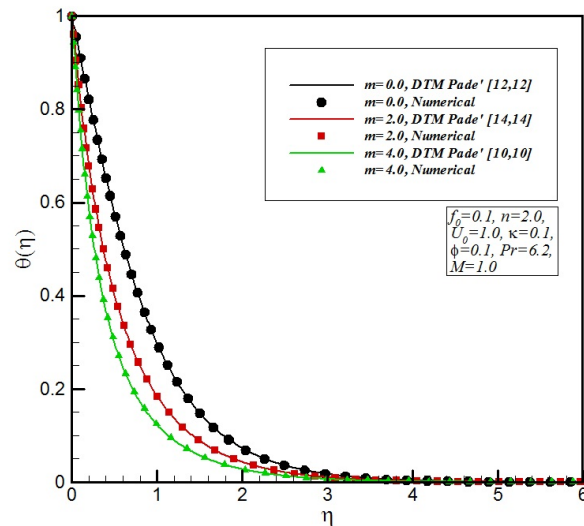


FIGURE 20. Effect of the type of nanoparticle on the dimensionless velocity profile obtained by the DTM-padé and numerical method.

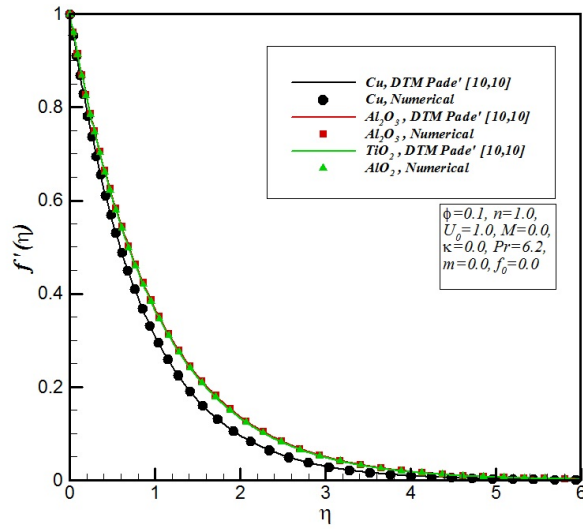


FIGURE 21. Effect of the type of nanoparticle on the dimensionless temperature profile obtained by the DTM-padé and numerical method.

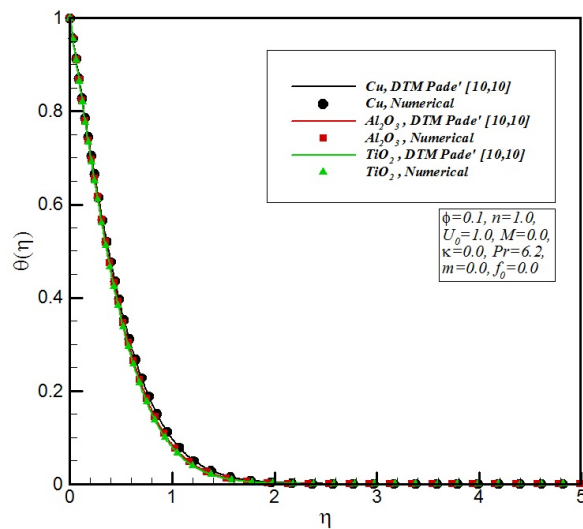


TABLE 1. Nomenclature

B_0	strength of magnetic field
C_f	skin friction factor
F	differential transform of f
f	dimensionless velocity functions
f_0	suction/injection parameter
K	permeability of the porous medium
k_f	thermal conductivity of base fluid
k_s	thermal conductivity of nanoparticle material
k_{nf}	effective thermal conductivity of nanofluid
M	magnetic parameter
m	nonlinear temperature parameter
n	nonlinear velocity parameter
Nu	Nusselt number
q_w	conduction heat transfer
T	Temperature
T_0	characteristic temperature
u	velocity in x -direction
U_0	stretching parameter
v	velocity in y -direction
x	distance along the surface
y	distance normal to the surface
Greek letters	
α_m	thermal diffusivity of the nanofluid
ϕ	solid volume fraction of the nanoparticles
η	similarity variable
τ_w	skin friction
μ_f	dynamic viscosity of base fluid
μ_{nf}	dynamic viscosity of nanofluid
Θ	differential transform of θ
θ	dimensionless temperature
σ	electric conductivity
ρ_f	density of base fluid
ρ_s	density of nanoparticle material
ρ_{nf}	density of nanofluid
$(\rho C)_f$	effective heat capacity of base fluid
$(\rho C)_s$	effective heat capacity of nanoparticle material
$(\rho C)_{nf}$	effective heat capacity of nanofluid
ν	kinematics viscosity
ψ	stream function
Subscript, Superscript	
∞	conditions far away from the surface
'	differentiation with respect to η
f	base fluid
s	nanoparticle material
nf	Nanofluid
w	Wall



TABLE 2. The operations for the one-dimensional differential transform method.

Original function	Transformed function
$w(x) = u(x) \pm v(x)$	$W(k) = U(k) \pm V(k)$
$w(x) = \lambda u(x)$	$W(k) = \lambda U(k), \lambda$ is a constant
$w(x) = x^r$	$W(k) = \delta(k - 1)$, where $\delta(k - 1) = \begin{cases} 1, & \text{if } k = r \\ 0, & \text{if } k \neq r \end{cases}$
$w(x) = \frac{du(x)}{dx}$	$W(k) = (k + 1)U(k + r)$
$w(x) = \frac{d^r u(x)}{dx^r}$	$W(k) = (k + 1)(k + 2)\dots(k + r)U(k + r)$
$w(x) = u(x)v(x)$	$W(k) = \sum_{r=0}^k U(r)V(k - r)$
$w(x) = \frac{du(x)}{dx} \frac{dv(x)}{dx}$	$W(k) = \sum_{r=0}^k (r + 1)(k - r + 1)U(r + 1)V(k - r + 1)$
$w(x) = u(x) \frac{dv(x)}{dx}$	$W(k) = \sum_{r=0}^k (k - r + 1)U(r)V(k - r + 1)$
$w(x) = u(x) \frac{dv(x)}{dx} \frac{dz(x)}{dx}$	$W(k) = \sum_{r=0}^k \sum_{t=0}^{k-r} (t + 1)(k - r - t + 1) \times U(r)V(t + 1)Z(k - r - t + 1)$

TABLE 3. Comparison of the results for the skin friction coefficient and the local Nusselt with those reported in Refs [50-53] for different values of n and f_0 when $\phi = 0, M = 0, \kappa = 0, Pr = 1.0$ and $m = 2n$.

Physical properties	Base fluid(water)	Cu	Al_2O_3	TiO_2
$C_p(J/kgK)$	4179	385	765	686.2
$\rho(kg/m^3)$	997.1	8933	3970	4250
$k(W/mK)$	0.613	400	40	8.954
$\alpha \times 10^{-7}(m^2/s)$	1.47	1163.1	131.7	30.7

TABLE 4. Thermophysical properties of the base fluid and the nanoparticles.

n	f_0	$f''(0)$				$\theta'(0)$			
		Cortell [13]	Rohni et al. [44]	Present Work		Cortell [13]	Rohni et al. [44]	Present work	
				Numerical	DTM-Padé			Numerical	DTM-Padé
0.75	-1	-1.63299	-1.633064	-1.63307	-1.63315	-1.25267	-1.25345	-1.25346	-1.25346
	0	-0.95379	-0.953957	-0.954021	-0.954023				
	1	-0.55015	-0.550158	-0.561477	-0.561467				
1.5	-1	-1.59316	-1.593215	-1.59322	-1.59332	-1.43939	-1.43938	-1.43937	-1.43937
	0	-1.06159	-1.061601	-1.06166	-1.06184				
	1	-0.71365	-0.713657	-0.723424	-0.723415				
10	-1	-1.45446	-1.454544	-1.45456	-1.45467	-1.728934	-1.728383	-1.72894	-1.72887
	0	-1.23488	-1.234875	-1.23493	-1.23491				
	1	-1.05367	-1.053678	-1.06785	-1.06779				



TABLE 5. Comparison of the results with those given by Hamad [20] for different values of ϕ and M for three different types of nanoparticle in the water when $f_0 = \kappa = m = 0.0$, $U_0 = n = 1.0$, $Pr = 6.2$.

M	ϕ	$f''(0)$			$\theta'(0)$			
		Cu	Al_2O_3	TiO_2	Cu	Al_2O_3	TiO_2	
0	0.1	Hamad [20]	-1.17475	-0.99877	-1.00952	-1.45207	-1.49170	-1.51959
		Present work	Numerical	-1.17476	-0.99872	-1.00954	-1.45201	-1.49175
	DTM-Padé		-1.17476	-0.99871	-1.00954	-1.45204	-1.49172	-1.51963
	0.2	Hamad [20]	-1.21804	-0.95592	-0.97259	-1.21290	-1.27118	-1.31805
		Present work	Numerical	-1.21806	-0.95596	-0.97262	-1.21289	-1.27119
	DTM-Padé		-1.21806	-0.95594	-0.97260	-1.21289	-1.27118	-1.31808
1	0.1	Hamad [20]	-1.46576	-1.32890	-1.33700	-1.38847	-1.41942	-1.44788
		Present work	Numerical	-1.46575	-1.32893	-1.33702	-1.38848	-1.41941
	DTM-Padé		-1.46575	-1.32892	-1.33702	-1.38849	-1.41942	-1.44790
	0.2	Hamad [20]	-1.43390	-1.21910	-1.23222	-1.16601	-1.21360	-1.26123
		Present work	Numerical	-1.43387	-1.21914	-1.23224	-1.16604	-1.21362
	DTM-Padé		-1.43387	-1.21917	-1.23223	-1.16602	-1.21362	-1.26124
2	0.1	Hamad [20]	-1.70789	-1.59198	-1.59875	-1.33600	-1.36212	-1.39085
		Present work	Numerical	-1.70792	-1.59199	-1.59876	-1.33602	-1.36214
	DTM-Padé		-1.70791	-1.59201	-1.59874	-1.33605	-1.36213	-1.39083
	0.2	Hamad [20]	-1.62126	-1.43480	-1.44596	-1.12582	-1.16675	-1.21474
		Present work	Numerical	-1.62127	-1.43486	-1.44598	-1.12584	-1.16677
	DTM-Padé		-1.62123	-1.43485	-1.44599	-1.12581	-1.16675	-1.2147

